Arabian Journal of Chemistry (2023) **16**, 104819

King Saud University

Arabian Journal of Chemistry

www.ksu.edu.sa
www.sciencedirect.com

ORIGINAL ARTICLE

Molecular recognition of tripeptides containing tryptophan by cucurbit[8]uril: A computational study

Osama M. Abuhasan [a], **Musa I. El-Barghouthi** [a,*], **Khaled Bodoor** [b,*], **Abdel Monem M. Rawashdeh** [c], **Khaleel I. Assaf** [d]

[a] *Department of Chemistry, Faculty of Science, The Hashemite University, P.O. Box 330127, Zarqa 13133, Jordan*
[b] *Department of Physics, The University of Jordan, Amman 11942, Jordan*
[c] *Department of Chemistry, Yarmouk University, Irbid 21163, Jordan*
[d] *Department of Chemistry, Faculty of Science, Al-Balqa Applied University, Al-Salt 19117, Jordan*

Received 26 December 2022; accepted 15 March 2023
Available online 22 March 2023

KEYWORDS

Cucurbit[8]uril;
Tripeptides;
Molecular recognition;
Molecular dynamics;
MM-PBSA;
TD-DFT;
Charge transfer complex

Abstract In this work, molecular dynamics (MD) simulations and time-dependent density functional theory (TD-DFT) calculations were applied to study the formation of binary and ternary complexes between cucurbit[8]uril (CB8) and three tryptophan-containing tripeptides (WGG, GWG, and GGW), as well as heteroternary complexes of the tripeptides in the presence of methyl viologen (MV) as an auxiliary ligand. All complexes were stable in water, and exhibited encapsulation of the indole moiety of W. Analysis of the MD trajectories of the homoternary complexes revealed π-π stacking within the CB8 cavity between the indole rings. MM-PBSA analysis indicated higher binding energy for tripeptides containing W residue at the N-terminus. The heteroternary complexes showed two binding modes, one with MV fully included (and π-π stacked with the indole ring) and the other with MV mostly excluded. The computed UV–Visible spectra of the free guests and their heteroternary complexes exhibited new bands emerged in the spectra of the complexes, which resulted from the transitions from HOMO and HOMO–1 to LUMO related to W–MV charge transfer (CT) complexes.

* Corresponding authors.
E-mail addresses: musab@hu.edu.jo (M.I. El-Barghouthi), kbodoor@ju.edu.jo (K. Bodoor).
Peer review under responsibility of King Saud University.

Production and hosting by Elsevier

https://doi.org/10.1016/j.arabjc.2023.104819
1878-5352

1. Introduction

Peptides are biomolecules that play central roles in many physiological processes. They act as neurotransmitters, neuromodulators, hormones and are involve in reproduction, metabolism and immune response (Sewald and Jakubke, 2009). Recognition of peptides by synthetic receptors has been studied, with implications for protein recognition and modulation and drug delivery (Broza et al., 2019; Das et al., 2019; Kubota and Hamachi, 2015; Smith et al., 2020; Smith and Royal Society of Chemistry (Great Britain), 2015). Several synthetic macrocyclic receptors with high affinity and selectivity toward amino acids (AAs), peptides and proteins have been studied, including cavitands (Pinalli et al., 2016), cyclodextrins (Buschmann et al., 2003), pillararenes (Duan et al., 2017; Li et al., 2013), calixarenes (Beshara et al., 2009; Da Silva and Coleman, 2003; Douteau-Guével et al., 2002, 1999; Mutihac et al., 2011; Nimse and Kim, 2013; Selkti et al., 2000), and cucurbiturils (Buschmann et al., 2003; Chinai et al., 2011; Gamal-Eldin and Macartney, 2013; Heitmann et al., 2006; Hirani et al., 2018; Rekharsky et al., 2008).

Cucurbit[*n*]urils (CB*n*, $n = 5$–8, 10, and 13–15) are a family of synthetic macrocycles receptors, where n represents the number of glycoluril units that are linked together by $2n$ methylene bridges. CB*n* homologues ($n = 5$–8) are known for their highly symmetrical structures, featuring a hydrophobic cavity and two polar portals, while larger homologues are folded into twisted shapes (Cheng et al., 2013; Li et al., 2016). CB*n* interact with cationic and neutral guest molecules via hydrogen bonding, ion–dipole and dipole–dipole interactions with the polar carbonyl rims, as well as the hydrophobic interaction within the cavity (Assaf and Nau, 2015; Biedermann et al., 2014, 2013, 2012).

CB*n* bind AAs (Bailey et al., 2008; Buschmann et al., 2003; Gamal-Eldin and Macartney, 2013; Lagona et al., 2006; Lee et al., 2015; Rajgariah and Urbach, 2008), peptides (Bush et al., 2005; Heitmann et al., 2006; Hirani et al., 2018; Rekharsky et al., 2008), and proteins (Chinai et al., 2011; Lei et al., 2010; Nguyen et al., 2010). Due to its small cavity size, CB6 can only form exclusion complexes with AAs, dipeptides, and tripeptides (Buschmann et al., 2005, 2003). In contrast, the cavity of CB7 was found to be more suitable to form inclusion complexes with AAs and peptides (Bailey et al., 2008; Lee et al., 2015; Rekharsky et al., 2006). Recognition of peptides by CB7 was found to be sequence selective; CB7 binds dipeptides containing aromatic residues more strongly when the residue is at the N-terminus than when it is at the C-terminus (Rekharsky et al., 2008). CB8 was found to bind aromatic AA and N-terminal aromatic peptides (Heitmann et al., 2006; Rajgariah and Urbach, 2008). Wu *et al*. studied the possible binding modes of peptides to CB8 by using diffusion-ordered NMR spectroscopy (DOSY) and demonstrated that dipeptides YL and FL can bind with CB8 in 1:1 and 2:1 stoichiometries based on the peptide to CB8 molar ratio (Wu et al., 2019). The 1:1 binding affinity of CB8 to methionine-terminated peptides was found to be affected by the neighboring AA (Hirani et al., 2018). The complexation of CB*n* with AAs and peptides was also studied by molecular dynamics (MD) simulations and quantum chemical calculations, providing additional structural and dynamic information (Bodoor et al., 2022, 2021; El-Barghouthi et al., 2022; Ma et al., 2021a, 2021b).

Heteroternary complexes were reported between CB8 and an AA or short peptide as one guest and an auxiliary ligand (AL), methyl viologen (MV) or tetramethyl benzobis(imidazolium) (MBBI), as the other (Biedermann et al., 2010; Bush et al., 2005; Ling et al., 2007). CB8:MV was found to bind tripeptides containing tryptophan (W) when W was at the N-terminus (WGG) more strongly than when W was in the middle or at the C-terminus (Bush et al., 2005). The binding of W-containing peptides to CB8:MV complex resulted in a strong charge transfer absorbance band (Bush et al., 2005). In order to further explore the effect of AA positions adjacent to W on the binding propensity of peptides to the CB8:MV complex, a library of 104 W-containing peptides (35 N-terminal W tripeptides and 69 non-terminal W pentapeptides was used (Ali et al., 2013). Results demonstrated a little or no effect on the identity of AA adjacent to W. A study on the complexation of tripeptides bearing N-terminal aromatic AA with CB8:MBBI was conducted, and results showed that peptides containing an N-terminal W bind to CB8:MBBI (forming heteroternary complex), while phenylalanine (F) peptides displace MBBI from the CB8 cavity (Smith et al., 2015a, 2015b). Most recently, using MD simulations CB7 was found to bind N-terminal leucine-containing tripeptides in aqueous solution more strongly than the corresponding N-terminal isoleucine-containing tripeptides (Zhao et al., 2023).

In this work, we employ MD simulations and time-dependent density functional theory (TD-DFT) calculations to computationally investigate for the first time the formation of binary and ternary complexes of CB8 with three W-containing tripeptides (WGG, GWG, and GGW). We also study the complexes of CB8 with the three tripeptides in the presence of MV. The Molecular Mechanics Poisson-Boltzmann surface area (MM-PBSA) method was used to calculate the non-covalent interactions between the host and guest(s) and evaluate the binding free energies, and to estimate the contribution of each AA to the binding energy. Conformational changes of the tripeptides upon complexation were inferred from their Ramachandran plots. TD-DFT calculations were utilized to study the charge-transfer (CT) interactions between the tripeptides and AL within CB8 and their effect on the UV–Visible absorption spectra.

2. Computational methods

MD simulations were performed using the pmemd.CUDA module of AMBER 16.0 (Case et al., 2016; Götz et al., 2012; Le Grand et al., 2013; Salomon-Ferrer et al., 2013), with the initial geometry of CB8 obtained from its X-ray structure (Kim et al., 2000). The force field used for the peptides was ff14SB (Maier et al., 2015), while for the for the ALs and CB8 it was General Amber Force Field (Wang et al., 2004). The RESP charges (Bayly et al., 1993) used for the MD simulations of CB8 and MV were computed to reproduce their electrostatic potentials, estimated using *ab initio* HF/6-31G* level of theory as applied in GAUSSIAN 16 software (Frisch et al., 2016). The TIP3P water model was used to solvate each system in a truncated octahedral periodic box (Jorgensen et al., 1983). The nonbonded interaction cutoff distance was set to 10.0 Å and the long-range electrostatic interactions were treated using the Particle Mesh Ewald (PME) method (York et al., 1993). The time step was set to 2 fs and SHAKE was applied to all bonds involving hydrogen atoms (Ryckaert et al., 1977). Top scoring complex geometries obtained using AutoDock Vina (Trott and Olson, 2009) were selected for a series of 40-ns MD simulations, which revealed that stable complexes for all tripeptides involved inclusion of W inside the CB8 cavity. Those stable complexes at the end of their 40 ns simulations were subsequently used as starting structures for simulations lasting 300 ns at 298.15 K and 1 atm. The average number of hydrogen bonds (HBs) was estimated using a cutoff distance $\leq$ 3.2 Å and a donor-hydrogen-acceptor cutoff angle $\geq 120^{\circ}$. Binding free energies (ΔG) were estimated using MM-PBSA (Homeyer and Gohlke, 2012) method via the MMPBSA.py script (Miller et al., 2012), according to the protocol described elsewhere (Dadou et al., 2017; El-Barghouthi et al., 2015, 2010).

DFT was used for geometry optimization of the heteroternary complexes in water, employing the Minnesota M06-2X functional (Mardirossian and Head-Gordon, 2016) and 6-31G(d,p) basis set (Becke, 1993; Lee et al., 1988) and the implicit universal solvation model based on density (SMD)

(Marenich et al., 2009). Vibrational frequency calculations were conducted and resulted in no negative eigenvalues. The time-dependent density functional theory (TD-DFT) (CASIDA, 1995; Runge and Gross, 1984) was used to calculate the lowest 20 singlet-to-singlet excitation energies.

3. Results and discussion

3.1. Binary and homoternary complexes

The average structures of the binary and homoternary complexes of the studied tripeptides with CB8, as computed from their 300-ns trajectories, are shown in Fig. 1. All binary complexes, irrespective of the position of W within the sequence, revealed the encapsulation of the hydrophobic side chain of W within the CB8 cavity (Fig. 1). The carboxylate group was excluded in the complexes of WGG and GWG, while in the complex of GGW, which exhibited two binding modes, it was included in one with a probability of 0.67 and excluded in the other with a probability of 0.33. Furthermore, the ammonium group in WGG complex was found to be in proximity to the CB8 portal, included in GWG complex, and in the bulk water away from the portal in GGW complex (Fig. 1). Similarly, the indole ring of W in the homoternary complexes of the tripeptides was encapsulated by CB8. The average numbers of water molecules within the CB8 cavity during the simulations of the binary complexes were 3, 0.5 and 2 for WGG, GWG and GGW, respectively. The largest desolvation of the CB8 cavity occurred for the binary complex of GWG, due to the inclusion of N-terminal G in addition to W (Fig. 1). Homoternary complexes exhibited complete expulsion of water from the cavity of CB8. Fig. 2 displays the probability distributions and density plots of the angle between the two planes of the indole rings within the homoternary complexes and the distance between their geometric centers. Evidence for π-π stacking comes from the averages for all complexes of the angle and distance (around 11° and 3.8 Å, respectively), which is further confirmed by the density plots. To form a qualitative picture of the favorable and unfavorable ion–dipole interactions of the above groups with the carbonyl portal, Fig. 3 depicts the positions sampled by the NH_3^+ and COO^- groups of the tripeptides in binary and ternary complexes. The NH_3^+ appears to be positioned for favorable ion–dipole interaction with the portals of CB8 in the complexes of WGG and GWG, and is expected to be largest for WGG due to its proximity to the carbonyl portal. In GGW, the NH_3^+ sampled positions far away above the carbonyl portal. As for the COO^-, in GGW it appeared to sample positions above the portal and within the cavity; in WGG and GWG it is above the portal, sampling further distances from the portal in WGG. The situation for the homoternary complex of WGG for both groups is qualitatively similar to its binary complex. As for the ternary complex of GWG, COO^- samples positions similar to those in the binary complex, whereas NH_3^+ is not included. For the ternary complex of GGW, COO^- is not included and NH_3^+ samples positions similar to those in the binary complex.

Fig. 4 displays the probability distributions of the end-to-end distance of each tripeptide in the free and bound states. The distributions are bimodal and very similar for the free tripeptides, irrespective of the amino acid sequence. In contrast, the tripeptides in the binary complexes sample conformations in which they are more extended: GWG and GGW the distance is largely constrained between 8 and 10 Å, while WGG samples a wider range of distances. Similarly, the two curves for the tripeptides in each ternary complexes display more extended conformations, which are nearly identical for WGG and GGW but shifted by ~ 1 Å for GWG.

Further insight into the conformational changes of the tripeptides associated with complex formation can be gained from Ramachandran plots (Fig. 5, and Fig. S1), which revealed that such changes are more pronounced for the complexes of GWG, since the position of W in the tripeptide in this case requires such changes for inclusion of W within the cavity of CB8.

The average numbers of HBs formed by each peptide in the free and bound states with water and the carbonyl portals of CB8 are shown in Fig. 6. and Fig. S2 and Table S1-S3. Compared to their free states, CB8 and tripeptides experienced a reduction in the number of HBs with water upon forming

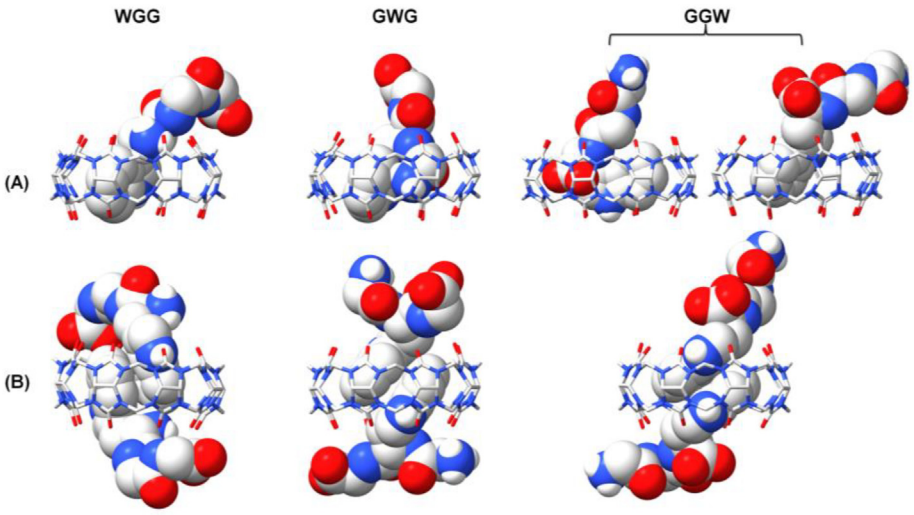

Fig. 1 Average structures of binary (A), homoternary (B) complexes of the studied tripeptides with CB8.

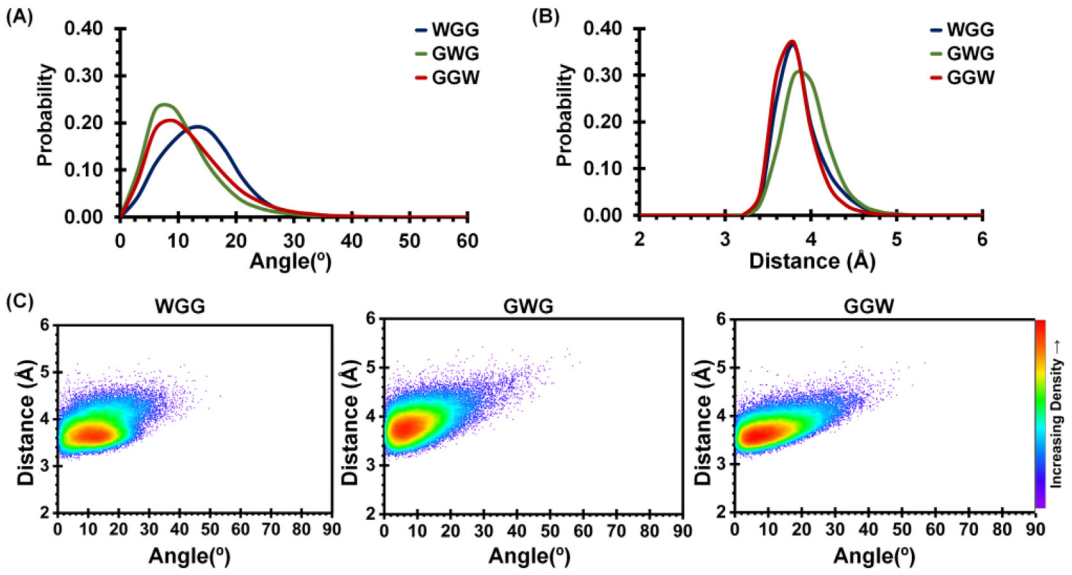

Fig. 2 π-π stacking of the homoternary complexes. Probability distributions of the angle between the two indole planes (A), Distances between centers of mass for the indole rings of the tripeptides in the homoternary complexes (B) and their density dot plots (C).

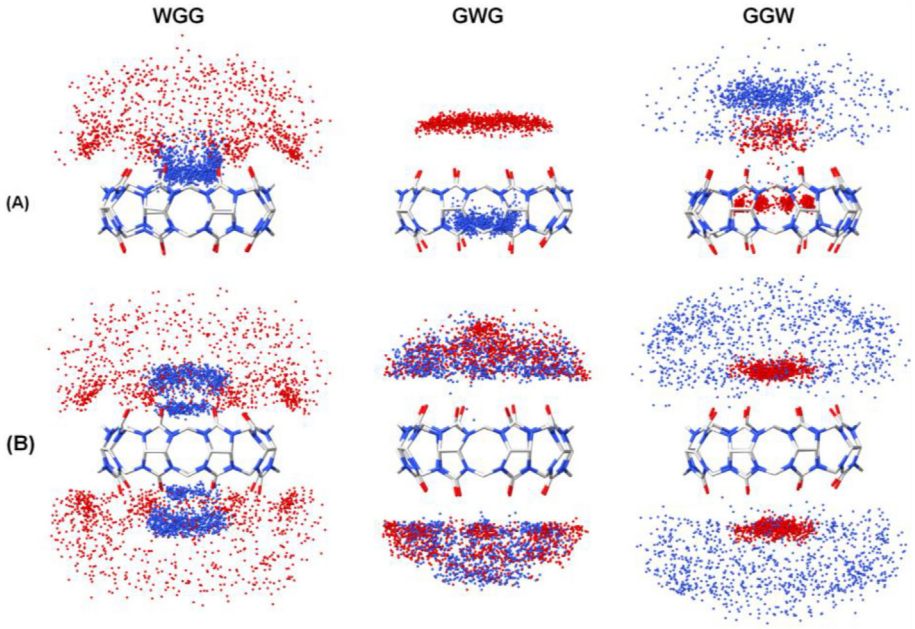

Fig. 3 Side views for the positions of the nitrogen atom in the N-terminus, and the carbon atom of carboxylate group in C-terminus (represented by dots colored with blue and red, respectively) within the binary (A), and homoternary (B) complexes (as extracted from 1000 equally spaced snapshots).

binary and ternary complexes; this reduction was partially compensated by new HBs formed between the terminal NH_3^+ and the side chain of W with CB8, with the numbers ordered according to WGG > GWG > GGW.

Table 1 displays the MM-PBSA estimates for the binding free energies and Fig. 7 (and Table S4) displays the contribution of each AA to the free energy. The van der Waals interaction for each complex ($\Delta\Delta E_{vdW}$), was favorable and mostly due to inclusion of W, as demonstrated by the free energy decomposition analysis (Fig. 7). The complex of WGG had the lowest vdW contribution among the binary complexes, since in the GWG and GGW complexes there were additional contributions from the inclusion of G and the COO^- group, respectively. The vdW contribution for the ternary complexes did not differ significantly. The electrostatic interaction (ΔE_{ELE}) to the binding free energy was favorable for all complexes, except for the homoternary complex of GGW, and appeared to be associated with the N-terminal residue (Fig. 7). The ΔE_{ELE} value for WGG was roughly twice that of GWG for both the binary and homoternary complexes.

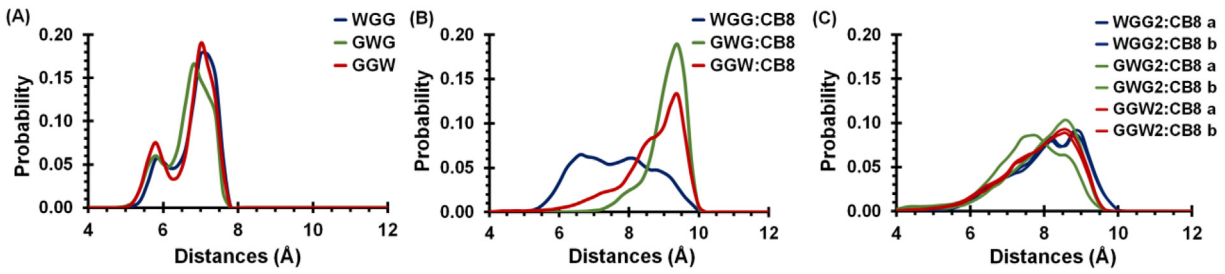

Fig. 4 Probability distributions of the distance between the N-terminus and C-terminus in free peptides (A), binary complexes (B), homoternary complexes (C).

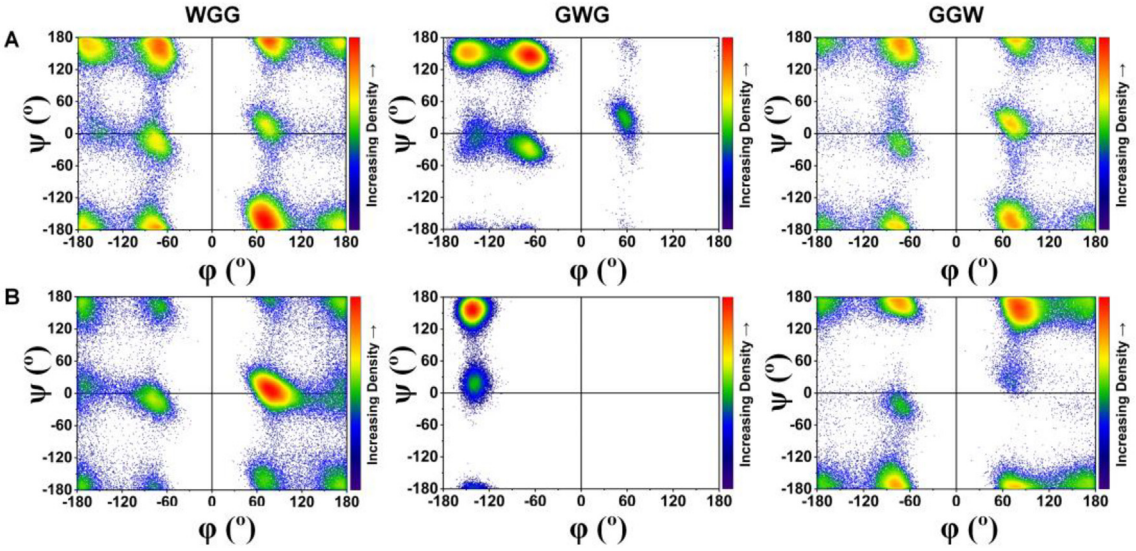

Fig. 5 Ramachandran distributions for the central residue in the A) free tripeptide B) tripeptide in the binary complex.

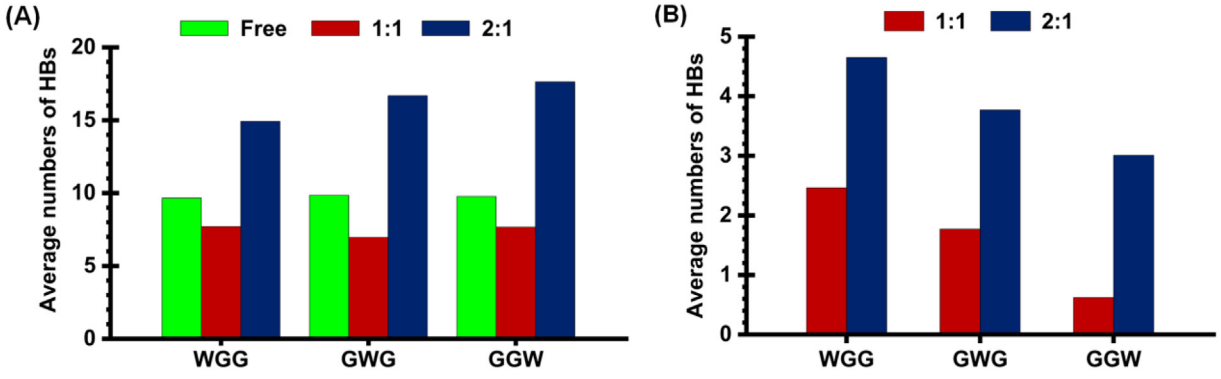

Fig. 6 Average numbers of HBs formed by peptides with water (A) and with CB8 (B).

While for GGW, the interaction had small favorable (unfavorable) contributions to the binary (homoternary) complexes. These contributions come from the interactions of NH_3^+ and COO^- with the carbonyl portal of CB8 and depend directly on the positions sampled by these groups (Fig. 3). The trend in the free energy of solvation (ΔG_{solv}) for the binary and ternary complexes appeared to be correlated with the extent of inclusion of NH_3^+ and COO^- and their interactions with CB8 (Fig. 3). The free binding energies (ΔG) were favorable for all binary and ternary complexes, with the trend for complex stability given by WGG > GWG > GGW; the differences were more pronounced for the ternary complexes, indicating a clear preference for CB8 to bind favorably with the tripeptide having an N-terminal W.

Comparing the values obtained in this work for the binding free energies of the (binary and ternary) complexes of CB8 with WGG and the previously obtained values (El-Barghouthi et al., 2022) of the corresponding complexes

Table 1 MM-PBSA estimates of the binding free energies (kcal·mol^{-1}) of binary and homoternary complexes.

		ΔE_{vdW}	ΔE_{ELE}	ΔG_{gas}	ΔG_{PB}	ΔG_{NP}	ΔG_{SOLV}	ΔG
Binary	WGG	−26.8	−39.3	−66.0	47.3	−3.7	43.5	−22.5
	GWG	−37.9	−20.1	−57.9	41.0	−4.1	36.9	−21.0
	GGW	−33.0	−4.7	−37.7	21.5	−3.8	17.7	−20.0
Homoternary	WGG	−57.2	−75.6	−132.8	96.1	−7.1	89.0	−43.8
	GWG	−54.7	−38.9	−93.6	66.1	−7.0	59.1	−34.4
	GGW	−53.1	9.7	−43.5	18.9	−6.6	12.3	−31.2

ΔE_{vdW} and ΔE_{ELE}: van der Waal and electrostatic energies as calculated from the molecular mechanics force field; $\Delta G_{gas} = \Delta E_{vdW} + \Delta E_{ELE}$; ΔG_{PB}: electrostatic contribution to the solvation free energy; ΔG_{NP}: non-polar contribution to the solvation free energy; $\Delta G_{SOLV} = \Delta G_{NP} + \Delta G_{PB}$; ΔG: estimated binding free energy as sum of the $\Delta G_{gas,}$ and ΔG_{SOLV}.

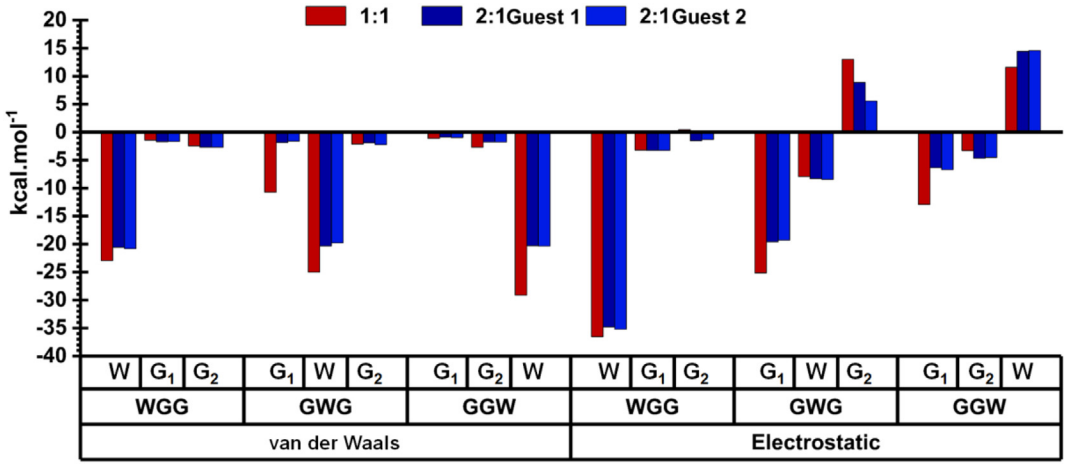

Fig. 7 van der waals and electrostatic contributions by each AA residue to the binding free energy in binary and homoternary complexes.

with the zwitterionic W, we see that the binary and ternary complexes of the WGG were more stable by ~ 7 and ~ 13 kcal·mol^{-1}, which might be due to the greater distance between COO^- and the carbonyl portal in the former.

3.2. Heteroternary complexes

MD simulations were also carried out for each tripeptide in complex with CB8 and the auxiliary ligand MV. Cluster analysis of the trajectories revealed two binding modes for each complex (Fig. 8), with the average structure for each mode exhibiting complete inclusion of the side chain of W, while MV appears encapsulated in one mode and almost excluded in the other. The heteroternary complexes of WGG, GWG and GGW had binding free energies of − 33.2, −30.1 and − 29.9 kcal·mol^{-1}, respectively. The above trend in the binding free energies agrees with the experimental one for the binding free energies of the corresponding tripeptides to the MV:CB8 complexes (Bush et al., 2005).

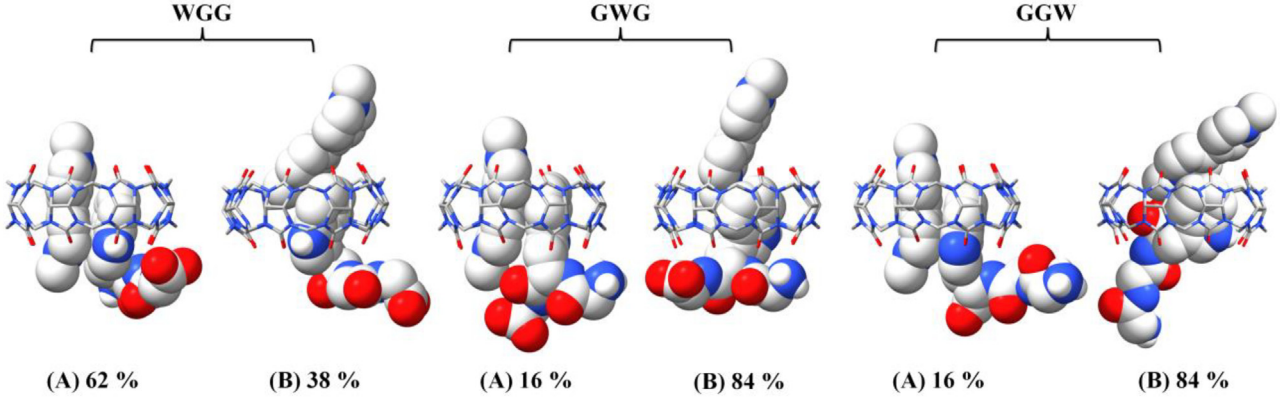

Fig. 8 Average structures of the ternary complexes of tripeptides with CB8 and MV.

The formation of CT complexes can be studied using UV–visible spectroscopy (Khan et al. 2020; Zulkarnain et al. 2017). Complex formation between W-containing peptides with CB8 in the presence of an auxiliary ligand (e.g., MV) resulted in the appearance of a charge-transfer band in the visible region (Bush et al., 2005; Ko et al., 2007). Therefore, TD-DFT calculations were performed to compute the UV–Visible spectra of the free tripeptides and MV and their ternary complexes with CB8. The input structures for the TD-DFT calculations were obtained from optimizing with DFT the MD-average structures of each binding mode (Fig. 8). The results (Table 2) revealed the appearance of two new transitions (HOMO → LUMO and HOMO − 1 → LUMO) for the tripeptide heteroternary complexes. For orientation-A complexes, the oscillator strength was larger for HOMO → LUMO than in the case of WGG, and for HOMO − 1 → LUMO for GWG and GGW. Oscillator strengths for the of the new transitions of orientation-B complexes were generally smaller in comparison with orientation A, because in the latter the orientation of the indole ring in the tripeptide with respect to MV is optimal for π-π stacking interaction.

The isodensity surface plots for HOMO − 1, HOMO and LUMO for the two orientations of the homoternary complexes are presented in Fig. 9 and Fig. S3. Contributions to HOMO – 1 and HOMO orbitals were mainly from the π orbital of the indole ring, with minor contribution from MV and G amino

Table 2 New transitions for the heteroternary complexes as obtained from TD-DFT.

Complex	Wavelength (nm)	Oscillator strength *(f)*	Major contribution
WGG:MV:CB8 (A)	421	0.0234	HOMO → LUMO (98%)
	365	0.0103	HOMO − 1 → LUMO (99%)
WGG:MV:CB8 (B)	389	0.0010	HOMO → LUMO (98%)
	340	0.0211	HOMO − 1 → LUMO (99%)
GWG:MV:CB8 (A)	418	0.0019	HOMO → LUMO (98%)
	358	0.0353	HOMO − 1 → LUMO (98%)
GWG:MV:CB8 (B)	380	0.0099	HOMO → LUMO (94%)
	332	0.0081	HOMO − 1 → LUMO (95%)
GGW:MV:CB8 (A)	453	0.0003	HOMO → LUMO (99%)
	370	0.0492	HOMO − 1 → LUMO (99%)
GGW:MV:CB8 (B)	377	0.0010	HOMO → LUMO (97%)
	330	0.0054	HOMO − 1 → LUMO (97%)

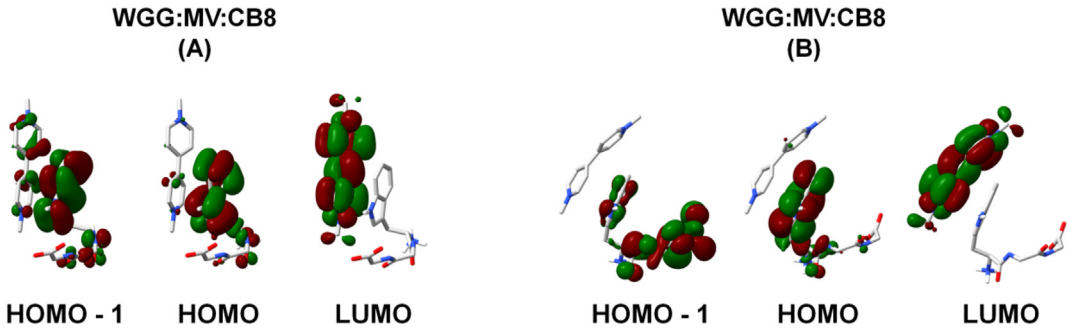

Fig. 9 Isodensity plots of HOMO − 1, HOMO and LUMO orbitals for WGG heteroternary complex in orientations A and B (CB8 removed for clarity).

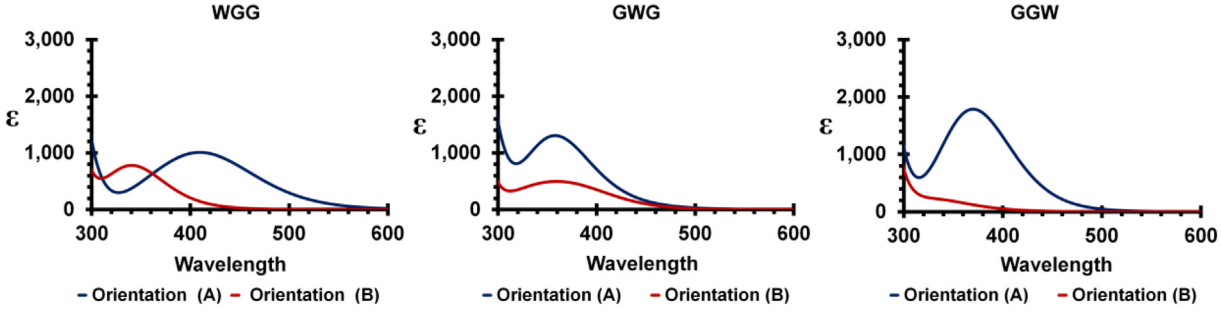

Fig. 10 Computed UV–Visible spectra of the heteroternary complexes.

acids in the case of HOMO – 1, while LUMO was found to be formed from the π* orbital of MV. Therefore, the new transitions found correspond to a charge-transfer band. The computed UV–Visible spectra are shown in Fig. 10 and Fig. S4, with λ_{max} for the CT bands of orientation A of WGG, GWG and GGW complexes at 420, 370 and 380 nm, respectively; the intensities of the new bands for orientation-B complexes were significantly lower.

4. Conclusion

MD simulations conducted in water in the presence and absence of MV revealed the formation of stable binary and ternary complexes between CB8 and three W-containing tripeptides, with the side chain of W encapsulated within the cavity of CB8. Ramachandran plots revealed conformational changes for the tripeptides upon complexation, especially for GWG. MM-PBSA results showed significant sequence-dependent variation among the binary and ternary complexes in the electrostatic contribution to their binding free energies, showing a preferential binding by CB8 to N-terminal-W tripeptide. Two modes of binding were found for the heteroternary complexes with an auxiliary ligand, in which the MV was included in one mode and mostly excluded in the other. TD-DFT calculations revealed new bands corresponding to charge transfer between the tripeptide and MV inside the cavity of CB8.

Declaration of Competing Interest

The authors declare that they have no known competing financial interests or personal relationships that could have appeared to influence the work reported in this paper.

Acknowledgment

The authors wish to acknowledge financial support from the Hashemite University.

Appendix A. Supplementary material

Supplementary data to this article can be found online at https://doi.org/10.1016/j.arabjc.2023.104819.

References

Ali, O.A., Olson, E.M., Urbach, A.R., 2013. Effects of sequence context on the binding of tryptophan-containing peptides by the cucurbit[8]uril–methyl viologen complex. Supramol. Chem. 25, 863–868. https://doi.org/10.1080/10610278.2013.810338.

Assaf, K.I., Nau, W.M., 2015. Cucurbiturils: from synthesis to high-affinity binding and catalysis. Chem. Soc. Rev. 44, 394–418. https://doi.org/10.1039/C4CS00273C.

Bailey, D.M., Hennig, A., Uzunova, V.D., Nau, W.M., 2008. Supramolecular tandem enzyme assays for multiparameter sensor arrays and enantiomeric excess determination of amino acids. Chem. – Eur. J. 14, 6069–6077. https://doi.org/10.1002/chem.200800463.

Bayly, C.I., Cieplak, P., Cornell, W., Kollman, P.A., 1993. A well-behaved electrostatic potential based method using charge restraints for deriving atomic charges: the RESP model. J. Phys. Chem. 97, 10269–10280. https://doi.org/10.1021/j100142a004.

Becke, A.D., 1993. Density-functional thermochemistry. III. The role of exact exchange. J. Chem. Phys. 98, 5648–5652. https://doi.org/10.1063/1.464913.

Beshara, C.S., Jones, C.E., Daze, K.D., Lilgert, B.J., Hof, F., 2009. A simple calixarene recognizes post-translationally methylated lysine. ChemBioChem 11, 63–66. https://doi.org/10.1002/cbic.200900633.

Biedermann, F., Rauwald, U., Cziferszky, M., Williams, K.A., Gann, L.D., Guo, B.Y., Urbach, A.R., Bielawski, C.W., Scherman, O.A., 2010. Benzobis(imidazolium)-Cucurbit[8]uril complexes for binding and sensing aromatic compounds in aqueous solution. Chem. – Eur. J. 16, 13716–13722. https://doi.org/10.1002/chem.201002274.

Biedermann, F., Uzunova, V.D., Scherman, O.A., Nau, W.M., De Simone, A., 2012. Release of high-energy water as an essential driving force for the high-affinity binding of cucurbit[n]urils. J. Am. Chem. Soc. 134, 15318–15323. https://doi.org/10.1021/ja303309e.

Biedermann, F., Vendruscolo, M., Scherman, O.A., De Simone, A., Nau, W.M., 2013. Cucurbit[8]uril and blue-box: high-energy water release overwhelms electrostatic interactions. J. Am. Chem. Soc. 135, 14879–14888. https://doi.org/10.1021/ja407951x.

Biedermann, F., Nau, W.M., Schneider, H.-J., 2014. The Hydrophobic effect revisited—Studies with supramolecular complexes imply high-energy water as a noncovalent driving force. Angew. Chem. Int. Ed. 53, 11158–11171. https://doi.org/10.1002/anie.201310958.

Bodoor, K., El-Barghouthi, M.I., Assaf, K.I., Al Hourani, B.J., Rawashdeh, A.M.M., Abuhasan, O.M., Alhamad, D.F., Abdel-Halim, H.M., 2021. A molecular dynamics study of the complexation of tryptophan, phenylalanine and tyrosine amino acids with cucurbit[7]uril. J. Incl. Phenom. Macrocycl. Chem. 102, 159–168. https://doi.org/10.1007/s10847-021-01113-2.

Bodoor, K., El-Barghouthi, M.I., Abuhasan, O.M., Rawashdeh, A.M. M., Assaf, K.I., Hourani, B.J.A., 2022. Molecular dynamics and TD-DFT study of the ternary complexes of cucurbit[8]uril with aromatic amino acids and auxiliary ligands. ChemistrySelect 7. https://doi.org/10.1002/slct.202201988.

Broza, Y.Y., Zhou, X., Yuan, M., Qu, D., Zheng, Y., Vishinkin, R., Khatib, M., Wu, W., Haick, H., 2019. Disease detection with molecular biomarkers: from chemistry of body fluids to nature-inspired chemical sensors. Chem. Rev. 119, 11761–11817. https://doi.org/10.1021/acs.chemrev.9b00437.

Buschmann, H.-J., Schollmeyer, E., Mutihac, L., 2003. The formation of amino acid and dipeptide complexes with α-cyclodextrin and cucurbit[6]uril in aqueous solutions studied by titration calorimetry. Thermochim. Acta 399, 203–208. https://doi.org/10.1016/S0040-6031(02)00462-8.

Buschmann, H.-J., Mutihac, L., Mutihac, R.-C., Schollmeyer, E., 2005. Complexation behavior of cucurbit[6]uril with short polypeptides. Thermochim. Acta 430, 79–82. https://doi.org/10.1016/j.tca.2005.01.002.

Bush, M.E., Bouley, N.D., Urbach, A.R., 2005. Charge-Mediated recognition of N-Terminal tryptophan in aqueous solution by a synthetic host. J. Am. Chem. Soc. 127, 14511–14517. https://doi.org/10.1021/ja0548440.

Case, D., Betz, R., Cerutti, D.S., Cheatham, T., Darden, T., Duke, R., Giese, T.J., Gohlke, H., Götz, A., Homeyer, N., Izadi, S., Janowski, P., Kaus, J., Kovalenko, A., Lee, T.-S., LeGrand, S., Li, P., Lin, C., Luchko, T., Kollman, P., 2016. Amber 16. University of California, San Francisco.

Casida, M.E., 1995. Time-Dependent Density Functional Response Theory for Molecules, in: Recent Advances in Density Functional Methods, Recent Advances in Computational Chemistry. World Scientific, pp. 155–192. https://doi.org/10.1142/9789812830586_0005.

Cheng, X.-J., Liang, L.-L., Chen, K., Ji, N.-N., Xiao, X., Zhang, J.-X., Zhang, Y.-Q., Xue, S.-F., Zhu, Q.-J., Ni, X.-L., Tao, Z., 2013. Twisted Cucurbit[14]uril. Angew. Chem. Int. Ed. 52, 7252–7255. https://doi.org/10.1002/anie.201210267.

Chinai, J.M., Taylor, A.B., Ryno, L.M., Hargreaves, N.D., Morris, C. A., Hart, P.J., Urbach, A.R., 2011. Molecular recognition of insulin by a synthetic receptor. J. Am. Chem. Soc. 133, 8810–8813. https://doi.org/10.1021/ja201581x.

Da Silva, E., Coleman, A.W., 2003. Synthesis and complexation properties towards amino acids of mono-substituted p-sulphonato-calix-[n]-arenes. Tetrahedron 59, 7357–7364. https://doi.org/10.1016/S0040-4020(03)01137-2.

Dadou, S., El-Barghouthi, M., Alabdallah, S., Badwan, A., Antonijevic, M., Chowdhry, B., 2017. Effect of protonation state and N-Acetylation of chitosan on its interaction with xanthan gum: a molecular dynamics simulation study. Mar. Drugs 15, 298. https://doi.org/10.3390/md15100298.

Das, D., Assaf, K.I., Nau, W.M., 2019. Applications of cucurbiturils in medicinal chemistry and chemical biology. Front. Chem. 7, 619. https://doi.org/10.3389/fchem.2019.00619.

Douteau-Guével, N., Coleman, W., Morel, J.-P., Morel-Desrosiers, N., 1999. Complexation of the basic amino acids lysine and arginine by three sulfonatocalix[n]arenes (n = 4, 6 and 8) in water: microcalorimetric determination of the Gibbs energies, enthalpies and entropies of complexation. J. Chem. Soc. Perkin Trans. 2, 629–634. https://doi.org/10.1039/A806855K.

Douteau-Guével, N., Perret, F., Coleman, A.W., Morel, J.-P., Morel-Desrosiers, N., 2002. Binding of dipeptides and tripeptides containing lysine or arginine by p-sulfonatocalixarenes in water: NMR and microcalorimetric studies. J. Chem. Soc. Perkin Trans. 2, 524–532. https://doi.org/10.1039/b109553f.

Duan, Q., Zhao, W., Lu, K., 2017. Synthesis of a water-soluble pillar[6]arene dodecaamine and its selective binding of acidic amino acids in water. Tetrahedron Lett. 58, 4403–4406. https://doi.org/10.1016/j.tetlet.2017.10.025.

El-Barghouthi, M.I., Assaf, K.I., Rawashdeh, A.M.M., 2010. Molecular dynamics of methyl viologen-cucurbit[n]uril complexes in aqueous solution. J. Chem. Theory Comput. 6, 984–992. https://doi.org/10.1021/ct900622h.

El-Barghouthi, M.I., Abdel-Halim, H.M., Haj-Ibrahim, F.J., Assaf, K. I., 2015. Molecular dynamics simulation study of the structural features and inclusion capacities of cucurbit[6]uril derivatives in aqueous solutions. Supramol. Chem. 27, 80–89. https://doi.org/10.1080/10610278.2014.910601.

El-Barghouthi, M.I., Bodoor, K., Abuhasan, O.M., Assaf, K.I., Al Hourani, B.J., Rawashdeh, A.M.M., 2022. Binary and ternary complexes of cucurbit[8]uril with tryptophan, phenylalanine, and tyrosine: a computational study. ACS Omega 7, 10729–10737. https://doi.org/10.1021/acsomega.2c00511.

Frisch, M.J., Trucks, G.W., Schlegel, H.B., Scuseria, G.E., Robb, M. A., Cheeseman, J.R., Scalmani, G., Barone, V., Petersson, G.A., Nakatsuji, H., Li, X., Caricato, M., Marenich, A.V., Bloino, J., Janesko, B.G., Gomperts, R., Mennucci, B., Hratchian, H.P., Ortiz, J.V., Izmaylov, A.F., Sonnenberg, J.L., Williams-Young, D., Ding, F., Lipparini, F., Egidi, F., Goings, J., Peng, B., Petrone, A., Henderson, T., Ranasinghe, D., Zakrzewski, V.G., Gao, J., Rega, N., Zheng, G., Liang, W., Hada, M., Ehara, M., Toyota, K., Fukuda, R., Hasegawa, J., Ishida, M., Nakajima, T., Honda, Y., Kitao, O., Nakai, H., Vreven, T., Throssell, K., Montgomery Jr., J. A., Peralta, J.E., Ogliaro, F., Bearpark, M.J., Heyd, J.J., Brothers, E.N., Kudin, K.N., Staroverov, V.N., Keith, T.A., Kobayashi, R., Normand, J., Raghavachari, K., Rendell, A.P., Burant, J.C., Iyengar, S.S., Tomasi, J., Cossi, M., Millam, J.M., Klene, M., Adamo, C., Cammi, R., Ochterski, J.W., Martin, R.L., Morokuma, K., Farkas, O., Foresman, J.B., Fox, D.J., 2016. Gaussian 16. Gaussian, Inc., Wallingford CT.

Gamal-Eldin, M.A., Macartney, D.H., 2013. Selective molecular recognition of methylated lysines and arginines by cucurbit[6]uril and cucurbit[7]uril in aqueous solution. Org. Biomol. Chem. 11, 488–495. https://doi.org/10.1039/C2OB27007B.

Götz, A.W., Williamson, M.J., Xu, D., Poole, D., Le Grand, S., Walker, R.C., 2012. Routine microsecond molecular dynamics simulations with AMBER on GPUs. 1. Generalized Born. J. Chem. Theory Comput. 8, 1542–1555. https://doi.org/10.1021/ct200909j.

Heitmann, L.M., Taylor, A.B., Hart, P.J., Urbach, A.R., 2006. Sequence-Specific recognition and cooperative dimerization of N-Terminal aromatic peptides in aqueous solution by a synthetic host. J. Am. Chem. Soc. 128, 12574–12581. https://doi.org/10.1021/ja064323s.

Hirani, Z., Taylor, H.F., Babcock, E.F., Bockus, A.T., Varnado, C.D., Bielawski, C.W., Urbach, A.R., 2018. Molecular recognition of methionine-terminated peptides by cucurbit[8]uril. J. Am. Chem. Soc. 140, 12263–12269. https://doi.org/10.1021/jacs.8b07865.

Homeyer, N., Gohlke, H., 2012. Free energy calculations by the molecular mechanics poisson−boltzmann surface area method. Mol. Inform. 31, 114–122. https://doi.org/10.1002/minf.201100135.

Jorgensen, W.L., Chandrasekhar, J., Madura, J.D., Impey, R.W., Klein, M.L., 1983. Comparison of simple potential functions for simulating liquid water. J. Chem. Phys. 79, 926–935. https://doi.org/10.1063/1.445869.

Khan, I.M., Alam, K., Afshan, M., Shakya, S., Islam, M., 2020. Thermodynamic and structural studies of newly prepared CT complex between pyrazole as a donor and salicylic acid as acceptor at various temperatures in ethanol. J. Mol. Struct. 1206,. https://doi.org/10.1016/j.molstruc.2020.127758 127758.

Kim, J., Jung, I.-S., Kim, S.-Y., Lee, E., Kang, J.-K., Sakamoto, S., Yamaguchi, K., Kim, K., 2000. New cucurbituril homologues: syntheses, isolation, characterization, and X-ray crystal structures of cucurbit[n]uril (n = 5, 7, and 8). J. Am. Chem. Soc. 122, 540–541. https://doi.org/10.1021/ja993376p.

Ko, Y.H., Kim, E., Hwang, I., Kim, K., 2007. Supramolecular assemblies built with host-stabilized charge-transfer interactions. Chem. Commun. 1305–1315. https://doi.org/10.1039/B615103E.

Kubota, R., Hamachi, I., 2015. Protein recognition using synthetic small-molecular binders toward optical protein sensing in vitro and in live cells. Chem. Soc. Rev. 44, 4454–4471. https://doi.org/10.1039/C4CS00381K.

Lagona, J., Wagner, B.D., Isaacs, L., 2006. Molecular-Recognition properties of a water-soluble cucurbit[6]uril analogue. J. Org. Chem. 71, 1181–1190. https://doi.org/10.1021/jo052294i.

Le Grand, S., Götz, A.W., Walker, R.C., 2013. SPFP: Speed without compromise—A mixed precision model for GPU accelerated molecular dynamics simulations. Comput. Phys. Commun. 184, 374–380. https://doi.org/10.1016/j.cpc.2012.09.022.

Lee, J.W., Lee, H.H.L., Ko, Y.H., Kim, K., Kim, H.I., 2015. Deciphering the specific high-affinity binding of cucurbit[7]uril to amino acids in water. J. Phys. Chem. B 119, 4628–4636. https://doi.org/10.1021/acs.jpcb.5b00743.

Lee, C., Yang, W., Parr, R.G., 1988. Development of the Colle-Salvetti correlation-energy formula into a functional of the electron density. Phys. Rev. B 37, 785–789. https://doi.org/10.1103/PhysRevB.37.785.

Lei, W., Jiang, G., Zhou, Q., Zhang, B., Wang, X., 2010. Greatly enhanced binding of a cationic porphyrin towards bovine serum albumin by cucurbit[8]uril. Phys. Chem. Chem. Phys. 12, 13255–13260. https://doi.org/10.1039/C001013H.

Li, C., Ma, J., Zhao, L., Zhang, Y., Yu, Y., Shu, X., Li, J., Jia, X., 2013. Molecular selective binding of basic amino acids by a water-soluble pillar[5]arene. Chem. Commun. 49, 1924. https://doi.org/10.1039/c3cc38622h.

Li, Q., Qiu, S.-C., Zhang, J., Chen, K., Huang, Y., Xiao, X., Zhang, Y., Li, F., Zhang, Y.-Q., Xue, S.-F., Zhu, Q.-J., Tao, Z., Lindoy, L. F., Wei, G., 2016. Twisted Cucurbit[n]urils. Org. Lett. 18, 4020–4023. https://doi.org/10.1021/acs.orglett.6b01842.

Ling, Y., Wang, W., Kaifer, A.E., 2007. A new cucurbit[8]uril-based fluorescent receptor for indole derivatives. Chem. Commun. 610–612. https://doi.org/10.1039/B611559D.

Ma, F., Zheng, X., Li, Z., 2021a. Sequence-selective recognition of cationic amphipathic tripeptides with similar structures in aqueous solutions by cucurbit[7]uril. Phys. Chem. Chem. Phys. 23, 13724–13733. https://doi.org/10.1039/D1CP01326B.

Ma, F., Zheng, X., Xie, L., Li, Z., 2021b. Sequence-dependent nanomolar binding of tripeptides containing N-terminal pheny-

lalanine by Cucurbit[7]uril: a theoretical study. J. Mol. Liq. 328,. https://doi.org/10.1016/j.molliq.2021.115479 115479.

Maier, J.A., Martinez, C., Kasavajhala, K., Wickstrom, L., Hauser, K. E., Simmerling, C., 2015. ff14SB: Improving the Accuracy of Protein Side Chain and Backbone Parameters from ff99SB. J. Chem. Theory Comput. 11, 3696–3713. https://doi.org/10.1021/acs.jctc.5b00255.

Mardirossian, N., Head-Gordon, M., 2016. How Accurate are the minnesota density functionals for noncovalent interactions, isomerization energies, thermochemistry, and barrier heights involving molecules composed of main-group elements? J. Chem. Theory Comput. 12, 4303–4325. https://doi.org/10.1021/acs.jctc.6b00637.

Marenich, A.V., Cramer, C.J., Truhlar, D.G., 2009. Universal solvation model based on solute electron density and on a continuum model of the solvent defined by the bulk dielectric constant and atomic surface tensions. J. Phys. Chem. B 113, 6378–6396. https://doi.org/10.1021/jp810292n.

Miller, B.R., McGee, T.D., Swails, J.M., Homeyer, N., Gohlke, H., Roitberg, A.E., 2012. MMPBSA.py: an efficient program for end-state free energy calculations. J. Chem. Theory Comput. 8, 3314–3321. https://doi.org/10.1021/ct300418h.

Mutihac, L., Lee, J.H., Kim, J.S., Vicens, J., 2011. Recognition of amino acids by functionalized calixarenes. Chem. Soc. Rev. 40, 2777–2796. https://doi.org/10.1039/C0CS00005A.

Nguyen, H.D., Dang, D.T., van Dongen, J.L.J., Brunsveld, L., 2010. Protein dimerization induced by supramolecular interactions with cucurbit[8]uril. Angew. Chem. Int. Ed. 49, 895–898. https://doi.org/10.1002/anie.200904413.

Nimse, S.B., Kim, T., 2013. Biological applications of functionalized calixarenes. Chem. Soc. Rev. 42, 366–386. https://doi.org/10.1039/C2CS35233H.

Pinalli, R., Brancatelli, G., Pedrini, A., Menozzi, D., Hernández, D., Ballester, P., Geremia, S., Dalcanale, E., 2016. The Origin of Selectivity in the complexation of N-Methyl amino acids by Tetraphosphonate Cavitands. J. Am. Chem. Soc. 138, 8569–8580. https://doi.org/10.1021/jacs.6b04372.

Rajgariah, P., Urbach, A.R., 2008. Scope of amino acid recognition by cucurbit[8]uril. J. Incl. Phenom. Macrocycl. Chem. 62, 251–254. https://doi.org/10.1007/s10847-008-9464-y.

Rekharsky, M.V., Yamamura, H., Inoue, C., Kawai, M., Osaka, I., Arakawa, R., Shiba, K., Sato, A., Ko, Y.H., Selvapalam, N., Kim, K., Inoue, Y., 2006. Chiral recognition in cucurbituril cavities. J. Am. Chem. Soc. 128, 14871–14880. https://doi.org/10.1021/ja063323p.

Rekharsky, M.V., Yamamura, H., Ko, Y.H., Selvapalam, N., Kim, K., Inoue, Y., 2008. Sequence recognition and self-sorting of a dipeptide by cucurbit[6]uril and cucurbit[7]uril. Chem. Commun. 2236–2238. https://doi.org/10.1039/B719902C.

Runge, E., Gross, E.K.U., 1984. Density-functional theory for time-dependent systems. Phys. Rev. Lett. 52, 997–1000. https://doi.org/10.1103/PhysRevLett.52.997.

Ryckaert, J.-P., Ciccotti, G., Berendsen, H.J.C., 1977. Numerical integration of the cartesian equations of motion of a system with constraints: molecular dynamics of n-alkanes. J. Comput. Phys. 23, 327–341. https://doi.org/10.1016/0021-9991(77)90098-5.

Salomon-Ferrer, R., Götz, A.W., Poole, D., Le Grand, S., Walker, R. C., 2013. Routine Microsecond Molecular Dynamics Simulations with AMBER on GPUs. 2. Explicit Solvent Particle Mesh Ewald. J. Chem. Theory Comput. 9, 3878–3888. https://doi.org/10.1021/ct400314y.

Selkti, M., Coleman, A.W., Nicolis, I., Douteau-Guével, N., Villain, F., Tomas, A., de Rango, C., 2000. The first example of a substrate spanning the calix[4]arene bilayer: the solid state complex of -sulfonatocalix[4]arene with -lysine. Chem Commun 161–162. https://doi.org/10.1039/A906546F.

Sewald, N., Jakubke, H.-D., 2009. Peptides: chemistry and biology. Wiley-VCH, Weinheim.

Smith, B.D., Royal Society of Chemistry (Great Britain) (Eds.), 2015. Synthetic receptors for biomolecules: design principles and applications, Monographs in supramolecular chemistry. Royal Society of Chemistry, Cambridge.

Smith, L.C., Leach, D.G., Blaylock, B.E., Ali, O.A., Urbach, A.R., 2015b. Sequence-Specific, Nanomolar Peptide Binding via Cucurbit[8]uril-Induced Folding and Inclusion of Neighboring Side Chains. J. Am. Chem. Soc. 137, 3663–3669. https://doi.org/10.1021/jacs.5b00718.

Smith, A.A.A., Maikawa, C.L., Roth, G.A., Appel, E.A., 2020. Site-selective modification of proteins using cucurbit[7]uril as supramolecular protection for *N* -terminal aromatic amino acids. Org. Biomol. Chem. 18, 4371–4375. https://doi.org/10.1039/D0OB01004A.

Trott, O., Olson, A.J., 2009. AutoDock Vina: Improving the speed and accuracy of docking with a new scoring function, efficient optimization, and multithreading. J. Comput. Chem. NA-NA. https://doi.org/10.1002/jcc.21334.

Wang, J., Wolf, R.M., Caldwell, J.W., Kollman, P.A., Case, D.A., 2004. Development and testing of a general amber force field. J. Comput. Chem. 25, 1157–1174. https://doi.org/10.1002/jcc.20035.

Wu, G., Clarke, D.E., Wu, C., Scherman, O.A., 2019. Oligopeptide-CB[8] complexation with switchable binding pathways. Org. Biomol. Chem. 17, 3514–3520. https://doi.org/10.1039/C9OB00592G.

York, D.M., Darden, T.A., Pedersen, L.G., 1993. The effect of long-range electrostatic interactions in simulations of macromolecular crystals: a comparison of the Ewald and truncated list methods. J. Chem. Phys. 99, 8345–8348. https://doi.org/10.1063/1.465608.

Zhao, Y., Li, F., Ma, F., Zhi, J., Wu, G., Zheng, X., 2023. Theoretical prediction of nanomolar and sequence-selective binding of synthetic supramolecular cucurbit[7]uril to N-terminal Leu-containing tripeptides. Phys. Chem. Chem. Phys. https://doi.org/10.1039/D2CP03818H.

Zulkarnain, Z., Khan, I.M., Ahmad, A., Miyan, L., Ahmad, M., Azizc, N., 2017. Synthesis of charge transfer complex of chloranilic acid as acceptor with p-nitroaniline as donor: Crystallographic, UV–visible spectrophotometric and antimicrobial studies. J. Mol. Struct. 1141, 687–697. https://doi.org/10.1016/j.molstruc.2017.03.050.